JOURNAL OF BACTERIOLOGY, Apr. 2007, p. 2886–2896 Vol. 189, No. 7
0021-9193/07/$08.00+0 doi:10.1128/JB.01767-06

σ^B Regulates IS*256*-Mediated *Staphylococcus aureus* Biofilm Phenotypic Variation[▽]

Jaione Valle,[1]† Marta Vergara-Irigaray,[1] Nekane Merino,[1] José R. Penadés,[2] and Iñigo Lasa[1]*

Laboratory of Microbial Biofilms, Instituto de Agrobiotecnología, and Departamento de Producción Agraria, Universidad Pública de Navarra-CSIC, Pamplona-31006, Spain,[1] and Instituto Valenciano de Investigaciones Agrarias (IVIA) and Cardenal Herrera-CEU University, 46113 Moncada, Valencia, Spain[2]

Received 20 November 2006/Accepted 23 January 2007

Biofilm formation in *Staphylococcus aureus* is subject to phase variation, and biofilm-negative derivatives emerge sporadically from a biofilm-positive bacterial population. To date, the only known mechanism for generating biofilm phenotypic variation in staphylococci is the reversible insertion/excision of IS*256* in biofilm-essential genes. In this study, we present evidence suggesting that the absence of the σ^B transcription factor dramatically increases the rate of switching to the biofilm-negative phenotype in the clinical isolate *S. aureus* 15981, under both steady-state and flow conditions. The phenotypic switching correlates with a dramatic increase in the number of IS*256* copies in the chromosomes of biofilm-negative variants, as well as with an augmented IS*256* insertion frequency into the *icaC* and the *sarA* genes. IS*256*-mediated biofilm switching is reversible, and biofilm-positive variants could emerge from biofilm-negative σ^B mutants. Analysis of the chromosomal insertion frequency using a recombinant IS*256* element tagged with an erythromycin marker showed an almost three-times-higher transposition frequency in a $\Delta\sigma^B$ strain. However, regulation of IS*256* activity by σ^B appears to be indirect, since transposase transcription is not affected in the absence of σ^B and IS*256* activity is inhibited to wild-type levels in a $\Delta\sigma^B$ strain under NaCl stress. Overall, our results identify a new role for σ^B as a negative regulator of insertion sequence transposition and support the idea that deregulation of IS*256* activity abrogates biofilm formation capacity in *S. aureus*.

Staphylococcus aureus is a leading cause of human diseases ranging from minor skin infections and food poisoning to life-threatening endocarditis, osteomyelitis, and postsurgical infections. In recent years, *S. aureus* has become one of the most important bacteria responsible for infections associated with the use of medical devices (47). The capacity of *S. aureus* to adhere to and form multilayered communities, termed "biofilms," on the surfaces of implanted devices appears to be one of the major causes of persistent infection following surgery (11, 43). Inside the biofilm, bacteria are embedded in a self-produced matrix that provides a stable protective environment and also acts as a nidus for the dissemination of cells that initiate recurrent infections (20).

Although much effort has been made to identify the essential genetic elements and regulatory mechanisms of *S. aureus* biofilm formation, little is known about the mechanisms underlying the dispersion of the bacteria from the mature biofilm. In a pioneering study, Ziebuhr et al. (48) showed that insertion/excision of the insertion sequence IS*256* in the *icaADBC* operon plays a direct role in the "on-to-off" switching of the biofilm formation capacity of *Staphylococcus epidermidis*. The *icaADBC* operon encodes proteins responsible for the synthesis of the PIA/PNAG (polysaccharide intercellular adhesin/polymeric *N*-acetyl glucosamine) exopolysaccharide, which is an important component of the staphylococcal biofilm matrix (12, 21, 35, 37). More recently, it was reported that IS*256* also contributes to the production of biofilm-negative variants of *S. epidermidis* through insertion/excision events in the *sarA* and *rsbU* genes (9). SarA, which controls the expression of over 100 genes, is required for *icaADBC* operon expression, PIA/PNAG synthesis, and biofilm development in *S. aureus* and *S. epidermidis* (4, 44, 45). The RsbU protein is a positive activator of the transcription factor σ^B, and its disruption is associated with the loss of biofilm-forming capacity in *S. epidermidis* (29). One question that remains is how an *S. epidermidis* cell is able to alter its IS*256* activity to allow adaptation of its biofilm-forming capacity to environmental conditions. Different host factors, including histone-like proteins (IHF, HU, HNS), Dam methylation, DNA supercoiling, proteins involved in DNA damage repair, proteases, and chaperones, have been described as important in regulating transposition (38). However, there is apparently no general rule governing transposition regulation, and each mobile element seems to have its own set of factors.

In a previous study in which we analyzed the biofilm formation capacity of the clinical strain *S. aureus* 15981, we observed that disruption of σ^B triggered the appearance of smooth colonies in the population (45). To corroborate this observation, in the present study we have investigated the biofilm phenotypic variation of the σ^B mutant under different growth conditions. Our results revealed that the absence of σ^B dramatically increased the rate of phenotypic switching to the biofilm-negative phenotype due to the increased transposition activity of IS*256*. Osmotic stress counteracted the absence of σ^B and restored the phenotypic switching of the σ^B mutant to levels similar to that of the wild-type strain. These results reveal strategies of the host cell for avoiding the adverse effects of the

* Corresponding author. Mailing address: Instituto de Agrobiotecnología, Universidad Pública de Navarra, Pamplona-31006, Spain. Phone: 34 948 168007. Fax: 34 948 232191. E-mail: ilasa@unavarra.es.
† Present address: Groupe de Génétique des Biofilms. Institut Pasteur, URA CNRS 2172, Paris 75724, France.
▽ Published ahead of print on 2 February 2007.

TABLE 1. Strains and plasmids used in this study

Strain or plasmid	Relevant characteristic(s)	Reference
Strains		
S. aureus		
15981	Biofilm-positive clinical strain	45
$\Delta\sigma^B$ strain	15981 $\Delta\sigma^B$	45
$\Delta\sigma^{B+}$ strain	15981 $\Delta\sigma^B$ with a restored σ^B gene	This study
icaC::Tn*917* strain	15981 *icaC*::Tn*917*	45
E. coli XL1-Blue	Used for cloning assays	
Plasmids		
pBT2	*E. coli-S. aureus* shuttle vector with a thermosensitive origin of replication for gram-positive bacteria	5
pMAD	*E. coli-S. aureus* shuttle vector with a thermosensitive origin of replication for gram-positive bacteria and the *bgaB* gene from *Bacillus stearothermophilus* encoding a thermostable β-galactosidase	1
pLA1	Plasmid that carries the IS*256* element containing the erythromycin cassette (IS*256*r)	This study
pLA1-ΔTnp	Plasmid that carries the IS*256*r element with a site-specifically mutated transposase	This study

excessive transposition of mobile elements and provide novel insights into the regulation of the transition from the planktonic to the biofilm lifestyle in *S. aureus*.

MATERIALS AND METHODS

Bacterial strains and culture conditions. The most relevant bacterial strains and plasmids used in this study are listed in Table 1. *Escherichia coli* XL1-Blue cells were grown in Luria-Bertani (LB) broth or on LB agar (Pronadisa, Spain) with appropriate antibiotics. Staphylococcal strains were cultured on Trypticase soy agar (TSA), in Trypticase soy broth (TSB) supplemented with 0.25% glucose (TSB-gluc), 0.5 M NaCl (TSB-NaCl), or 0.5 M KCl (TSB-KCl) where indicated. Media were supplemented with the following appropriate antibiotics at the indicated concentrations: erythromycin at 20 μg ml^{-1} or 1.5 μg ml^{-1}, ampicillin at 100 μg ml^{-1}, and chloramphenicol at 20 μg ml^{-1}.

Genetic manipulations. General DNA manipulations were performed by standard procedures (3). For σ^B restoration, the σ^B gene was amplified using the sigB-A and sigB-D primers from *S. aureus* 15981 (Table 2). The 1,064-bp fragment was cloned in the pGEM-T Easy vector (Promega). The fragment was then cloned into the BamHI site of the shuttle plasmid pMAD (1), and the resulting plasmid was transformed into the $\Delta\sigma^B$ strain by electroporation, using a previously described protocol (13). Allelic exchange in the absence of a selection marker was performed as previously described (2). Briefly, the pMAD plasmid harboring a wild-type copy of the σ^B gene was integrated into the chromosome through homologous recombination at a nonpermissive temperature (43.5°C). From the 43.5°C plate, one to five colonies were picked, placed into 3 ml of TSB-gluc, and incubated for 24 h at 30°C. Tenfold serial dilutions of this culture were plated on TSA containing X-Gal (5-bromo-4-chloro-3-indolyl-β-D-galactopyranoside) (1.5 μg/ml). White colonies, which no longer contained the pMAD plasmid, were tested to confirm the replacement by PCR using the sigB-A and sigB-D primers.

DNA hybridization for the detection of the *icaADBC* operon, IS*256*, and a recombinant IS*256* element (IS*256*r) was performed according to the protocol supplied with a PCR-digoxigenin DNA-labeling and chemiluminescence detection kit (Roche). The oligonucleotide pairs IS-1/IS-2, ISeri-3/ISica-4, and IcaA1-IcaA2 were used to generate the specific IS*256*, erythromycin gene, and *ica* operon probes.

For the measurement of IS*256* insertions in the *ica* operon, single rough colonies of the wild-type strain and the $\Delta\sigma^B$ mutant were cultured overnight in 5 ml of TSB-gluc. Then, dilutions were plated on Congo red agar (CRA). Biofilm-positive variants display a rough colony morphology when grown on this medium, whereas biofilm-negative variants exhibit a smooth colony morphology. One hundred ten smooth colonies of the wild-type strain and the $\Delta\sigma^B$ mutant were subjected to PCR for their *ica* genes using primers icaA-1/icaA-2, icaC-1/icaC-2, and icaB-1/icaD-2. The nucleotide sequencing was determined by the dideoxy chain termination method, using an ABI PRISM 310 genetic analyzer (Applied Biosystems).

Screening for biofilm-negative variants. Screening for biofilm-negative variants was performed on CRA (16). Strains were incubated overnight in 5 ml of TSB-gluc. Then, cultures were diluted 1:1,000 in 5 ml of TSB-gluc to continue the serial passage. After 5 days, a dilution was plated on CRA and incubated for 24 h at 37°C. To analyze the effect of environmental conditions on biofilm phenotypic variation, the strains were serially diluted in 5 ml of TSB, TSB-gluc, TSB-NaCl, and TSB-KCl at both 30 and 37°C for 5 days, and then the morphology on CRA plates was determined. The phenotypic variation on solid media was analyzed as follows. A single colony from each strain was resuspended in 20 μl of TSB. Five microliters of the resuspension was spotted on a TSA plate and incubated overnight. The next day, all of the colony was resuspended in 20 μl of TSB, and again 5 μl of the resuspension was spotted on a TSA plate to continue the serial passage. After 5 days, dilutions were plated on CRA and incubated for 24 h at

TABLE 2. Oligonucleotides used in this study

Oligonucleotide	Sequence
icaA-1	CTAACGAAAGGTAGGTA
icaA-2	AAGTGCTGTTTCTCTTAC
icaC-1	GGGACGGATTCCATGAAA
icaC-2	CGAAGTCGTCAATTCAAAC
icaB-1	CCGAACTCCAATGATTAT
IcaD-2	CTTATACAAATGCGACGG
sigB-A	GCAGTGTTAATACTGCTTC
sigB-D	GTTAATGAAGGAACGGAGG
sar1	GCTTTGAGTTGTTATCAAT
sar2	CGTTGTTTGCTTCAGTGA
sarC	TTCACCAAATTGCGCTAAACCCTCCCTATTTGATGCATCTTGCT
sarD	ACCCGTTATCAATCGG
IS-1	CCGACAAAGTCAACGAAA
IS-2	GGCTGATGTTTGATTGGG
ISica-1	CATTGTATTATCCTCAAATATATTTGATAAAGTCCGTATAATTG
ISeri-2	GTCGACCTATACAATGTTTTTACCA
ISeri-3	GGGTCGACCTATTGTGAGTTATTAGTG
ISica4	TCATTGTTTGCATATACAAATATATAGTCAAGTCCAGACTCCTGTGTAAAATAGTATAACTATTAGG
Iscir-1	CTCATAATAGCCATTTCGTTG
Iscir-2	GCTTGCGCATCATTGGATG
Tnp-Fw	GGATTCGAAGACGCCTTTCAA
Tnp-Rv	GATTCAGTCGTTCAATTAGATTGGTACTC
Gyr-Fw	ACGTATGAAGGTGGTACGCATG
Gyr-Rv	ACGCGTTAATGCACGTTTGA
icaTaq-Fw	ATCGGTGGCGACTTTGATCT
icaTaq-Rv	CGGCATCAGTCATAATGACGATT
GyrTaq-Fw	TGTGATTTTTGGTACACCTTGCTT
GyrTaq-Rv	AGGTGACTTTTTGGTAATTCAAGGTT
Tnp-3	CCATGGCTAAGTTAATATCTGTGAAC
Tnp-4	CCATGGCGCATCATTGGATGATGG

37°C. The ratio of smooth to rough colonies was determined. The frequency at which biofilm-negative variants were produced from a biofilm-forming colony (number of CFU per cell) was determined and generation was calculated as previously described (30).

Selection of biofilm-positive revertants. A single colony of a biofilm-negative variant was isolated and incubated at 37°C in TSB-gluc in 96-well polystyrene microtiter plates. After 24 h, the medium was replaced. This procedure was repeated until a biofilm of adhering bacteria became visible (around day 4). The adhering bacterial cells were scratched from the bottom and streaked on CRA. Rough colonies were isolated, and their capacity to produce a biofilm was determined by the quantitative adherence assay.

PNAG detection. PNAG production in *S. aureus* 15981, in the $\Delta\sigma^B$ strain, and in the biofilm-negative variants was detected as described previously (12). Cells were grown overnight in TSB-gluc, the optical density was determined, and the same number of cells of each culture was resuspended in 50 μl of 0.5 M EDTA (pH 8.0). Cells were incubated for 5 min at 100°C and then centrifuged to pellet them. Forty microliters of the supernatant was incubated with 10 μl of proteinase K (20 mg/ml; Sigma) for 30 min at 37°C. After the addition of 10 μl of Tris-buffered saline (20 mM Tris-HCl, 150 mM NaCl [pH 7.4]) containing 0.01% bromophenol blue, 5 μl was spotted on a nitrocellulose filter using a Bio-Dot microfiltration apparatus (Bio-Rad), blocked overnight with 5% skim milk in phosphate-buffered saline with 0.1% Tween 20, and incubated for 2 hours with an anti-*S. aureus* PNAG antibody diluted 1:10,000 (36). Bound antibodies were detected with peroxidase-conjugated goat anti-rabbit immunoglobulin G antibodies (Jackson ImmunoResearch Laboratories, Inc., PA) diluted 1:10,000 and the Amersham ECL Western blotting system.

Biofilm formation assays. A biofilm formation assay in microtiter wells was performed as described previously (21). To analyze the biofilm formation under flow conditions, we used 60-ml microfermentors with a continuous flow of 40 ml h^{-1} of TSB-gluc. Submerged Pyrex slides served as the growth substratum. Bacteria (10^8) from overnight precultures of wild-type 15981 and the $\Delta\sigma^B$ strain grown in TSB-gluc were used to inoculate microfermentors and subsequently cultivated for 5 days at 37°C. Biofilm development was recorded with a Nikon Coolpix 950 digital camera. To quantify the biofilm, bacteria that adhered to the Pyrex slide were resuspended in 10 ml of TSB. The optical density of the suspension was determined at 650 nm.

Detection of phenotypic variants in coagulases, lipases, proteases, and hemolysins. Strain 15981 and the $\Delta\sigma^B$ strain were incubated overnight in 5 ml of TSB-gluc. Then, cultures were diluted 1:1,000 in 5 ml of TSB-gluc to continue the serial passages. After 5 days of subcultivation, a dilution was plated on Baird Parker agar (Difco), Spirit Blue agar (Difco), TSA supplemented with skim milk (5%, wt/vol), and TSA with 5% sheep blood (Difco) to determine the number of colonies with phenotypic variations in coagulase, lipase, protease, and hemolysin production, respectively. For the detection of IS*256* insertions in the *sarA* gene, a dilution of an overnight culture of the wild type and the $\Delta\sigma^B$ mutants was plated on TSA-milk. After 24 h of incubation, the protease-overproducing variants were selected and PCR for the *sarA* gene performed using the sar1/sar2 and sarC/sarD primers.

Real-time quantitative PCR. Total *S. aureus* RNA was isolated using the Fast RNA-Blue kit (Bio 101) according to the manufacturer's instructions. Two micrograms of each RNA was subjected in duplicate to DNase I (Gibco-BRL) treatment for 30 min at 37°C. The enzyme was then inactivated at 65°C in the presence of EDTA. To verify the absence of genomic DNA in every sample, the RNA duplicates were reverse transcribed in the presence and absence of Moloney murine leukemia virus reverse transcriptase (Gibco-BRL) (RT-PCR). All preparations were purified using CentriSep spin columns (Princeton Separations, Adelphia, NJ). To measure IS*256* transposase (*tnp*) expression, 1/20 of each reaction mixture was used for real-time quantitative PCR (RT-PCR) using an ABI PRISM model 9700HT apparatus (Applied Biosystems). The *tnp* transcript was amplified using primers Tnp-Fw and Tnp-Rv (Table 2). The *gyrB* transcript was amplified as the endogenous control using primers Gyr-Fw and Gyr-Rv. SYBER green was used to label the amplified DNA. To monitor the specificity, final PCR products were analyzed by determining melting curves and by electrophoresis. Only samples with no amplification of the minus reverse transcriptase aliquot were considered in the study. The amount of *tnp* transcript was expressed as the difference (*n*-fold) from the amount of the control gene ($2^{-\Delta CT}$, where ΔC_T represents the difference in threshold cycle between the target and control genes). For *ica* expression, TaqMan probes were used (Applied Biosystems). The *icaC* transcripts were amplified using the primers icaTaqFw and icaTaqRv and the *icaC*-specific TaqMan probe.

Transposition activity of the IS*256*r element. To generate the recombinant element IS*256*r, the chromosomal *icaC*::IS*256* insertion from the $\Delta\sigma^B$ biofilm variant L-24 was amplified by PCR using primers ISica-1 and ISeri-2 (Table 2). The erythromycin resistance gene was amplified using primers ISeri-3 and ISica-4 (Table 2). Both fragments were fused, generating a recombinant element (IS*256*r). IS*256*r contains an erythromycin resistance gene as a selected marker and maintains intact both inverted repeats and the transposase gene. IS*256*r was cloned into the thermosensitive *E. coli-Staphylococcus* shuttle vector pBT2 (5), generating plasmid pLA1. Plasmid pLA1 was introduced into the *S. aureus* 15981 wild type and $\Delta\sigma^B$ mutant by electroporation. To construct the plasmid pLA1-ΔTnp, the *tnp* gene of the IS*256*r element was mutated using primers tnp-3 and tnp-4, which generate a deletion of 64 bp (Table 2). Mutated IS*256* was fused with the erythromycin resistance gene, generating the IS*256*rΔTnp recombinant element. IS*256*rΔTnp was cloned into pBT2, generating plasmid pLA1-ΔTnp.

Extrachromosomal template DNA from *E. coli* strains carrying pLA1 and pLA1-ΔTnp was prepared as previously described (34). IS*256* circle junctions were detected using primers Iscir1 and Iscir2 (Table 2), which are directed in opposite orientations.

To analyze the transposition activity of IS*256*r in each strain, transformants were grown at 28°C for 5 to 7 h to allow recombinant element transposition and then spread at 43°C (temperature nonpermissive for plasmid replication). The frequency of transposition was determined as the number of erythromycin-resistant and chloramphenicol-sensitive colonies.

Statistical analysis. Data corresponding to gene expression were compared using the Mann-Whitney test. Data corresponding to the frequency of transposition of the recombinant element IS*256*r were compared using the Pearson χ^2 test. All the tests were two sided, and the significance level was 5%. The statistical analysis was performed with the SPSS program.

RESULTS

Effect of σ^B on biofilm phenotypic variation. In a previous study, we demonstrated that the σ^B-null mutation in *S. aureus* did not impair the biofilm formation capacity of the 15981 clinical isolate (45). However, we realized that after several passages, the $\Delta\sigma^B$ mutant lost the capacity to produce a biofilm. To investigate whether σ^B regulates biofilm phenotype switching, a single rough colony each of the parent and $\Delta\sigma^B$ mutant strains was subcultured in TSB-gluc broth for 7 days as described in Materials and Methods. A dilution of each culture was plated daily on CRA plates, and the numbers of rough and smooth colonies were determined. *S. aureus* biofilm-negative derivatives are easily recognized on CRA plates because they produce smooth colonies, whereas biofilm-positive colonies are rough (Fig. 1A). In the $\Delta\sigma^B$ strain, the percentage of rough colonies changed dramatically from 97% at day 1 to 2 to 5% at day 7, while the percentage of rough colonies changed from 99.5% at day 1 to 95% at day 7 in the wild-type strain (Fig. 1B). To confirm that the biofilm phenotypic variation was a consequence of σ^B deletion, the σ^B gene was restored in the $\Delta\sigma^B$ mutant by allelic exchange. The restored strain ($\Delta\sigma^{B+}$) exhibited switching frequencies identical to those of the wild-type 15981 strain after serial passage, confirming that the increased biofilm instability was indeed due to σ^B deficiency (data not shown).

Analyses of the growth rate and the number of viable cells in smooth and rough variants indicated no difference in growth capacity that could explain the enrichment in smooth variants after 7 days (data not shown). However, to exclude the possibility that our experimental procedure in liquid media could artificially enrich smooth colonies in the $\Delta\sigma^B$ strain, we repeated the experiment on solid TSA plates as described in Materials and Methods. The results confirmed that the biofilm phenotype instability of the $\Delta\sigma^B$ strain also occurs after serial passage in solid medium (data not shown).

Biofilm phenotypic variation of the $\Delta\sigma^B$ mutant in microfermentors. Biofilm formation in microfermentors occurs un-

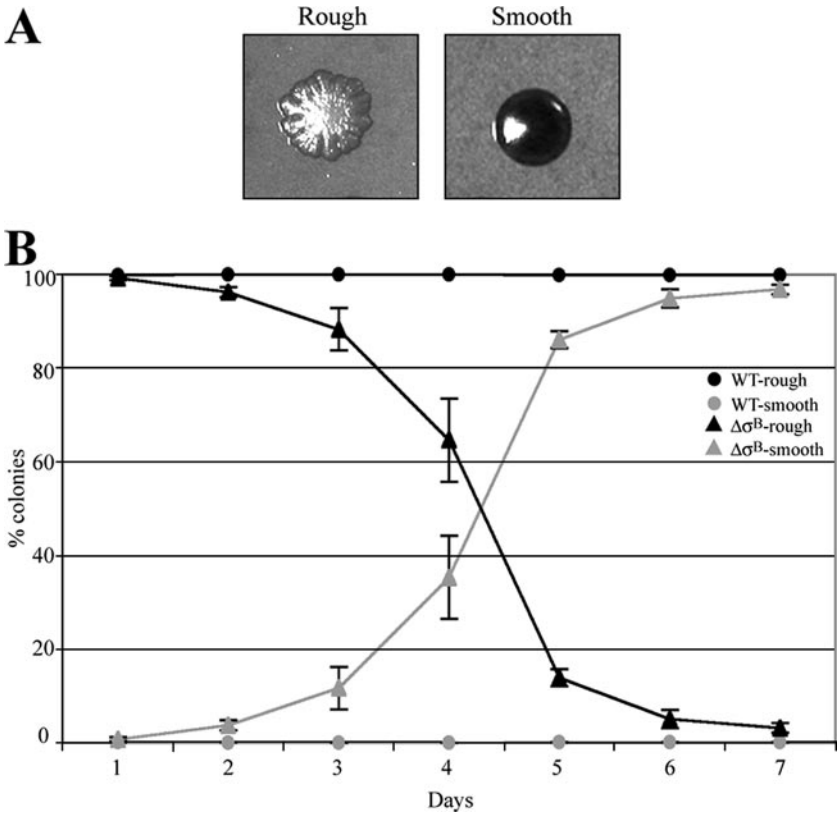

FIG. 1. Mutation of σ^B in a biofilm-positive strain causes a phenotype switch to a smooth morphology. (A) Colony morphology of biofilm-positive variants (rough morphology) and biofilm-negative variants (smooth morphology) of *S. aureus* 15981 after 24 h on CRA. (B) Percentages of rough colonies (black) and smooth colonies (gray) of the *S. aureus* 15981 strain and its isogenic $\Delta\sigma^B$ mutant on CRA after subcultivation in TSB-gluc for 7 days. Error bars represent the standard deviations from three independent experiments.

der flow conditions with a continuous replenishment of medium to avoid stationary phase. We used microfermentors to examine whether the rapid biofilm phenotypic switching of the $\Delta\sigma^B$ strain also occurs under flow conditions. The wild-type and $\Delta\sigma^B$ mutant strains were grown in microfermentors, and biofilm development was monitored over a period of 5 days. After 24 h, visual inspection of the biofilm revealed no difference in biofilm development between the parent and the $\Delta\sigma^B$ strain (Fig. 2A). However, after 5 days, the biofilm biomass produced by the $\Delta\sigma^B$ mutant was reduced twofold, and only a sparse layer of cells covered the surface of the slide (Fig. 2B). These data suggest that nutrient depletion and/or accumulation of waste products during steady-state incubation was not responsible for the induction of the rapid phenotypic switching observed in the $\Delta\sigma^B$ strain. These results also showed that the rapid enrichment of smooth bacteria in the $\Delta\sigma^B$ strain affects the three-dimensional structure of the biofilm.

Contribution of IS*256* to rapid biofilm switching in the $\Delta\sigma^B$ strain. The insertion/excision activity of the IS*256* transposable element in biofilm-essential genes has been described as a mechanism of biofilm phase variation (48). To determine whether the transposition activity of IS*256* was involved in the rapid phenotypic switching observed in the $\Delta\sigma^B$ strain, we performed Southern blot analysis using a probe specific for IS*256*. Figure 3 shows that new DNA bands detected by the IS*256* probe appeared as the $\Delta\sigma^B$ strain was serially passaged

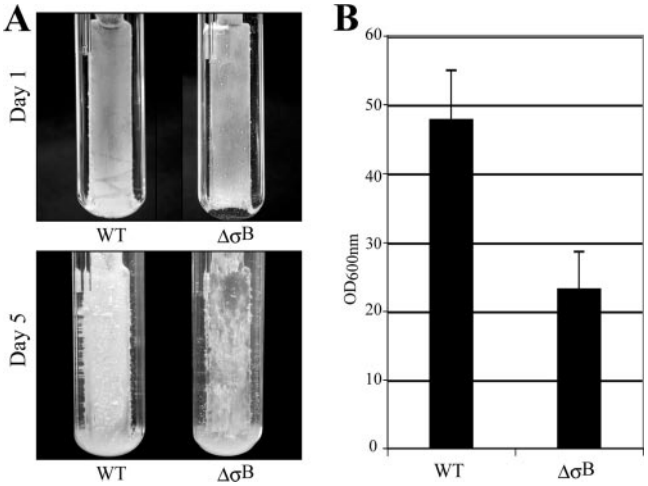

FIG. 2. Influence of σ^B deletion on biofilm stability after 5 days in continuous-flow microfermentors. (A) Biofilm development of the wild-type strain (WT) and the $\Delta\sigma^B$ mutant in microfermentors after 24 h (upper panel) and 5 days (lower panel). (B) Quantification of the biomass of a 5-day biofilm adhering to a glass slide. Cells were removed from the glass slide, placed into 10 ml of TSB, and vortexed, and the optical density (OD) of the solution was measured at 600 nm. Error bars represent the standard deviations from three independent experiments.

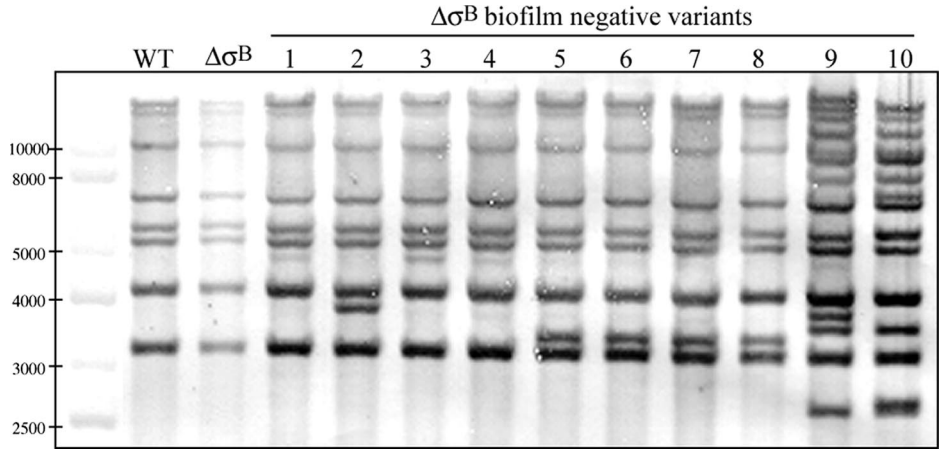

FIG. 3. Analysis of the IS*256* element in biofilm-negative variants of the $\Delta\sigma^B$ strain. Southern hybridization of EcoRI-SalI-digested chromosomal DNA with an IS*256*-specific DNA probe. Lanes 1 to 4, $\Delta\sigma^B$ biofilm-negative variants obtained from overnight cultures of experiment 1; lanes 5 to 8, $\Delta\sigma^B$ biofilm-negative variants obtained from overnight cultures of experiment 2; lanes 9 to 10, $\Delta\sigma^B$ biofilm-negative variants obtained after 7 days of subcultivation of the $\Delta\sigma^B$ mutant in TSB-gluc. WT, wild type.

in the laboratory. After 7 days, the number of copies of IS*256* increased dramatically, suggesting that the transposition activity of IS*256* was derepressed in the absence of σ^B.

This finding suggested that the insertion of new copies of IS*256* into the *icaADBC* operon is a likely mechanism for the rapid biofilm-negative switching of the $\Delta\sigma^B$ strain. To explore this possibility, we characterized the *icaADBC* operons of several biofilm-negative variants by Southern blotting and by PCR. Southern blot experiments using a probe specific for the *icaA* gene revealed three different hybridization patterns (Fig. 4A and B). Group I included biofilm-negative variants (smooth colonies) with hybridization patterns identical to that of the parental biofilm-positive $\Delta\sigma^B$ strain. These variants were unable to produce the PIA/PNAG exopolysaccharide (Fig. 4C), although transcription of the *icaADBC* operon showed no difference from that of the wild-type strain, as determined by RT-PCR using an *icaC*-specific TaqMan probe (data not shown). Biofilm formation of these biofilm-negative variants was restored by complementation with a recombinant plasmid carrying the *icaADBC* operon (pSC18), suggesting that a point mutation in the *ica* operon might be responsible for biofilm deficiency. Group III included biofilm-negative variants exhibiting a DNA band with a lower electrophoretic mobility than those of the parental biofilm-positive $\Delta\sigma^B$ strain. Biofilm-neg-

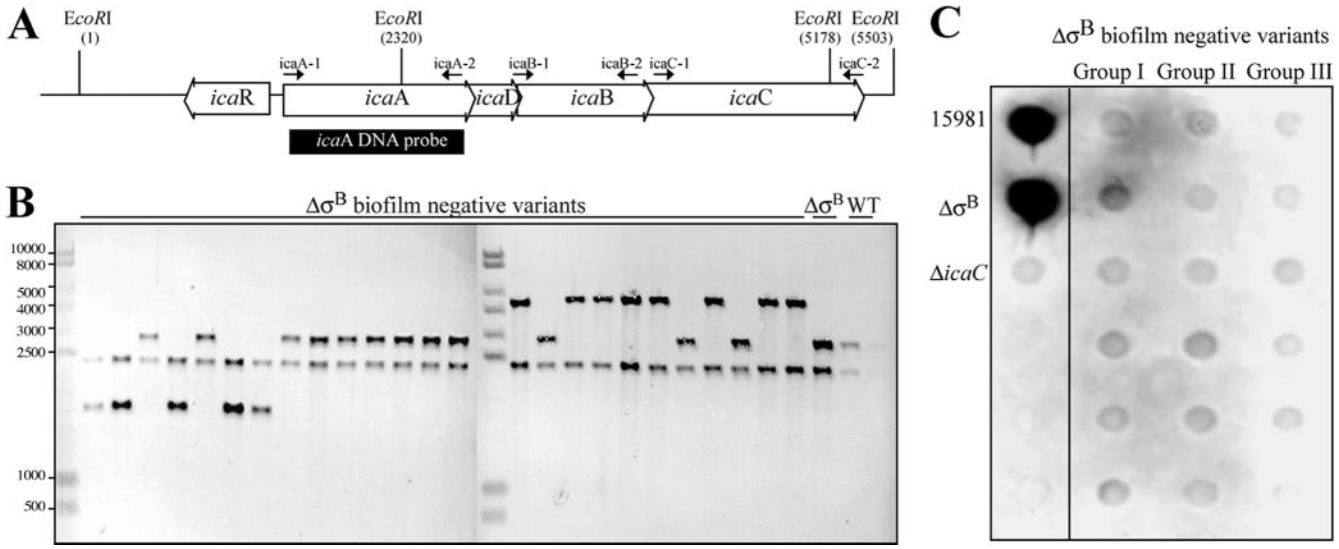

FIG. 4. Analysis of the *ica* operon of biofilm-negative variants of the $\Delta\sigma^B$ strain. (A) Scheme of the *ica* operon EcoRI restriction sites. The *icaA* DNA probe was generated using primers icaA-1 and icaA-2. (B) Southern blot analysis of EcoRI-digested chromosomal DNA of several $\Delta\sigma^B$ biofilm-negative variants using the amplified *icaA* DNA probe. WT, wild type. (C) Dot blot analysis of PNAG accumulation in the 15981 wild-type strain, the $\Delta\sigma^B$ strain, and the $\Delta\sigma^B$ biofilm-negative variants that were classified into group I (no insertion of IS*256* in the *ica* operon), group II (*icaC*::IS*256*), and group III (*icaC* deletion). Cell surface extracts of stationary-phase cultures were treated with proteinase K and spotted onto nitrocellulose filters. PNAG production was detected with anti-*S. aureus* PNAG antiserum. The transposon insertion mutation in the *icaC* gene was used as a negative control.

TABLE 3. Localization of IS*256* insertions in the *icaC* gene

$\Delta\sigma^B$ biofilm-negative variant	Position	Sequence[a]
8	381	TTTATCGTTG*TTATCATGCA
23	432	ATTAACTATA*ACCTATTCAA
29	417	ATATCATTTT*TAAAATTAAC
37	848	TTCTCATTCT*TTATTTATTT
53	933	GTCTTTCTAG*CGATATCACT
20	844	TGCTTTCTCA*TTCTTTATTT
22	405	TTATTTTGAG*TTATATCATT
24	906	ACAAATATAT*TTGAGGATAA
25	405	TTATTTTGAG*TTATATCATT

[a] * represents the insertion point of IS*256*.

ative variants of group II showed a hybridized band of higher electrophoretic mobility than was observed for bands in the parental strain. To investigate more precisely the reasons for the band shifts observed in biofilm mutants of groups II and III, the *ica* genes of several colonies were amplified by PCR and sequenced. The results revealed that the increased size of the *ica* restriction fragment of variants of group II was due to the insertion of the IS*256* element at different positions of the *icaC* gene (Table 3). To determine the frequency at which IS*256* insertions occurred in *icaC*, we performed PCR analysis of 110 biofilm-negative variants from the wild-type and $\Delta\sigma^B$ strains. The results revealed that 27 of the variants from the $\Delta\sigma^B$ strain contained an *icaC*::IS*256* insertion. In contrast, only three of the biofilm-negative variants derived from the wild-type strain contained an IS*256* insertion at the *ica* operon. The decreased size of the hybridized band of group III variants was due to a deletion of *icaC* and the DNA region downstream of the *icaADBC* operon because we were unable to amplify the *icaC* gene in these variants. As expected, dot blot experiments using specific anti-PNAG polyclonal antisera showed that all of the biofilm-negative smooth variants were unable to synthesize PIA/PNAG (Fig. 4C).

IS*256*-mediated biofilm phenotypic variation in the $\Delta\sigma^B$ strain is a reversible process. To determine whether the $\Delta\sigma^B$ biofilm-negative variants could revert to biofilm-positive phenotypes, representative biofilm-negative derivatives were serially subcultured in TSB-gluc broth for 5 days as described in Materials and Methods. Rough black colonies were isolated on CRA after 4 days. Southern hybridization with an IS*256*-specific DNA probe of several biofilm-positive revertants revealed decreases in the numbers of copies of IS*256* in the biofilm-positive revertants (Fig. 5A). In addition, rough colonies regained the capacity to produce a biofilm in microtiter plates (Fig. 5B) and to synthesize PIA/PNAG exopolysaccharide (Fig. 5C). Consistent with previous results by Ziebuhr et al. (48) for *S. epidermidis*, these data suggest that insertion of IS*256* in the *icaC* gene of $\Delta\sigma^B$ biofilm-negative variants is a reversible process.

IS*256* insertions outside the *ica* operon. In a previous study, Conlon et al. (9) reported that the *sarA* gene was another chromosomal hot spot for IS*256* insertions, leading to the generation of biofilm-negative variants. Therefore, we decided to analyze the frequency of insertion of IS*256* in the *sarA* gene in the $\Delta\sigma^B$ mutant. For this purpose, we took advantage of the fact that proteases are upregulated in the *sarA* mutant (7). A single colony each of the wild-type and $\Delta\sigma^B$ mutant strains was grown overnight in TSB-gluc. Then, an aliquot of each culture was plated daily on TSA-milk. The results of three independent experiments revealed that switching frequencies to protease-overproducing variants were 10 times higher for the $\Delta\sigma^B$ mutant than for the wild-type strain. PCR analysis of 34 of the $\Delta\sigma^B$ protease-overproducing variants revealed that 9 (26%) contained *sarA*::IS*256* insertions but that none of the 9 protease-overproducing variants obtained from the wild-type strain contained *sarA*::IS*256* insertions. Interestingly, all of the protease-overproducing variants containing *sarA*::IS*256* insertions had a reduced capacity to produce biofilms, whereas some of the protease-overproducing variants obtained from the wild-type strain still retained the capacity to produce a biofilm (data not shown).

Although insertion of IS*256* has been correlated only with biofilm phenotype switching, we wondered whether increased IS*256* insertion activity might also play a role in the variation of other phenotypes. We analyzed the frequency of switching for enzymatic activities easily detectable on agar plates, such as coagulase, α-hemolysin, and lipase production. After 5 days of subcultivation, we were unable to detect any phenotypic variants in coagulase, hemolysin, or lipase production (Fig. 6). Taken together, these data suggest that insertion of IS*256* into the *sarA* gene occurs at frequencies similar to that of the *ica*C gene, but insertion does not randomly occur in all genes of the staphylococcal genome.

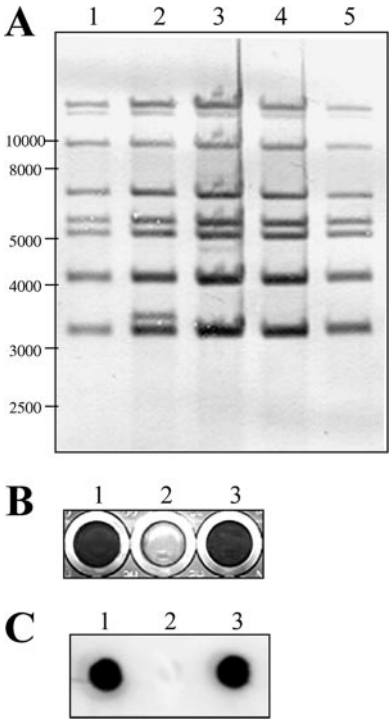

FIG. 5. Analysis of the IS*256* element, the biofilm formation capacity, and PIA/PNAG synthesis in $\Delta\sigma^B$ biofilm-positive revertants. (A) Southern hybridization of EcoRI-SalI-digested chromosomal DNA with an IS*256*-specific DNA probe. Lanes: 1, *S. aureus* 15981 $\Delta\sigma^B$ strain; 2, *S. aureus* 15981 $\Delta\sigma^B$ biofilm-negative variant; 3 to 5, *S. aureus* 15981 $\Delta\sigma^B$ biofilm-positive revertants. (B) Biofilm formation in microtiter dishes. (C) Dot blot analysis of PIA/PNAG accumulation.

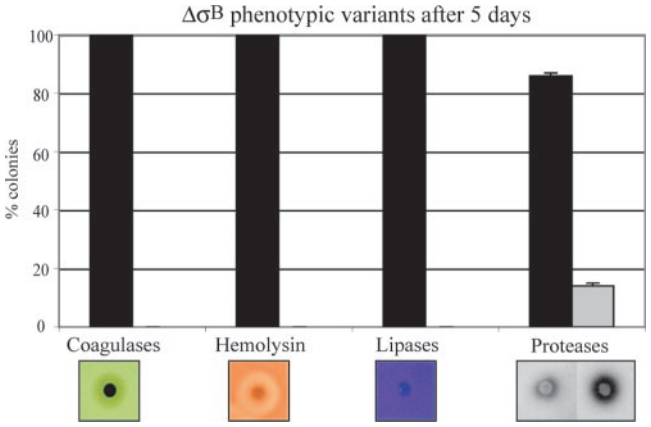

FIG. 6. Detection of phenotypic variants in coagulases, hemolysins, lipases, and proteases. After 5 days of subcultivation, a dilution of $\Delta\sigma^B$ biofilm-negative variant culture was plated on Baird Parker agar (Difco), TSA with 5% sheep blood (Difco), Spirit Blue agar (Difco), or TSA supplemented with skim milk (5%, wt/vol) to determine the number of phenotypic variants in coagulase, hemolysin, lipase, or protease production, respectively. The percentage of colonies that did not present phenotypic variation is represented in black. The percentage of colonies with phenotypic variation is shown in gray.

σ^B deficiency does not affect transposase expression. To investigate the possibility that σ^B affects IS*256* by regulating the expression of the transposase, we measured the transcription levels of the IS*256* transposase in wild-type and $\Delta\sigma^B$ strains by RT-PCR. This analysis revealed no significant differences in transposase transcription levels between the wild-type and the $\Delta\sigma^B$ mutant strains (data not shown). These results suggest that σ^B influences the activity of IS*256* by a mechanism other than repression of transcription of the transposase.

Recombinant IS*256* exhibits high insertion activity in a $\Delta\sigma^B$ strain. To determine whether the increased frequency of insertion of IS*256* was due to a higher IS*256* activity in the $\Delta\sigma^B$ mutant, we generated IS*256*r by insertion of an erythromycin resistance gene downstream of the transposase gene (Fig. 7A). IS*256*r was cloned into the thermosensitive pBT2 vector (5), generating pLA1. We also generated a derivative of IS*256*r in which the transposase gene was inactivated by site-directed mutagenesis of the conserved DDE motif. IS*256*r-ΔTnp was cloned into pBT2, generating pLA1-ΔTnp. To determine whether the transposase of IS*256*r was functional and capable of inducing IS*256*r excision and circularization, pLA1 and pLA1-ΔTnp were cloned in the recombination-deficient host *E. coli* XL1-Blue. For visualization of IS*256*r circles, extrach-

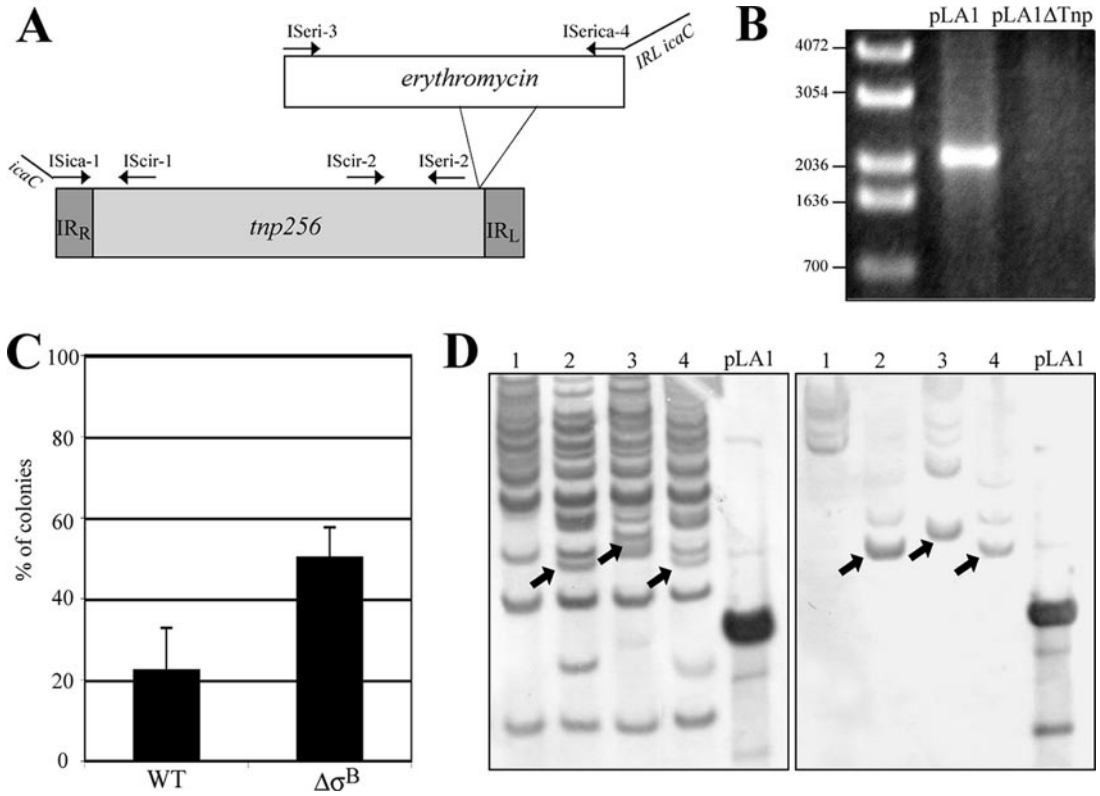

FIG. 7. Transposition analysis of the recombinant element IS*256*r. (A) Construction of the recombinant element IS*256*r. The natural chromosomal *icaC*::IS*256* insertion was amplified and fused with an erythromycin resistance gene that included the left inverted repeat (IR_L) of the IS*256* element. IS*256*r was cloned into the pBT2 vector. IR_R, right inverted repeat. (B) Agarose gel electrophoresis of PCR fragments amplified with circle-specific, outward-directed primers. (C) Percentages of chloramphenicol-sensitive colonies among the erythromycin-resistant colonies of *S. aureus* 15981 and its isogenic $\Delta\sigma^B$ mutant. Error bars represent the standard deviations from nine independent experiments. WT, wild type. (D) Southern hybridization of EcoRI-NcoI-digested chromosomal DNA with IS*256* (left)- and erythromycin (right)-specific DNA probes. The arrows indicate new DNA bands hybridizing with the IS*256* and erythromycin probes. Lanes 1 to 4, erythromycin-resistant/chloramphenicol-sensitive derivatives obtained from the $\Delta\sigma^B$ strain.

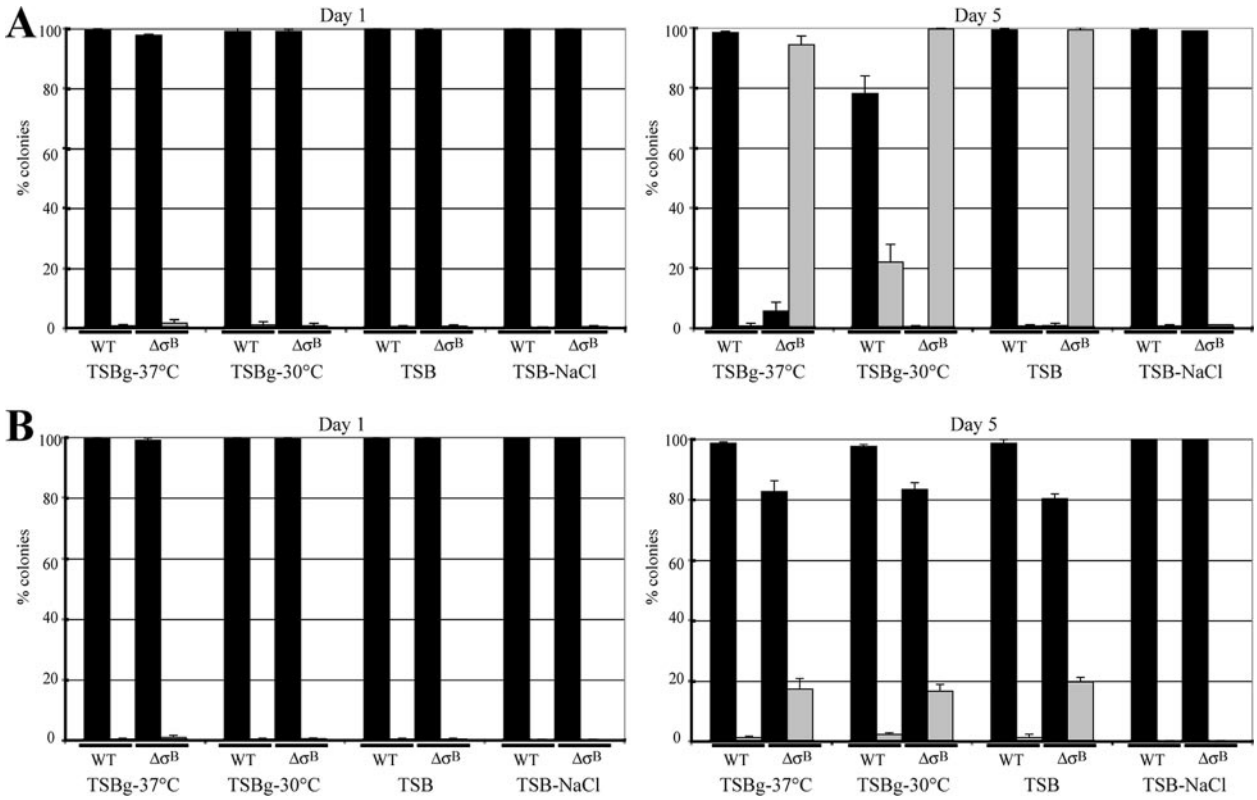

FIG. 8. Effect of culture media and temperature on IS*256* activity in the $\Delta\sigma^B$ strain. (A) Percentages of rough colonies (black) and smooth colonies (gray) of wild-type and $\Delta\sigma^B$ strains on CRA at days 1 and 5 of continuous subcultivation under different conditions (at 30°C or 37°C) and in TSB, TSB-gluc (TSBg), or TSB-NaCl. (B) Percentages of protease-overproducing colonies (black) and non-protease-overproducing colonies (gray) of wild-type and $\Delta\sigma^B$ strains on TSA-milk at days 1 and 5 of subcultivation under different conditions as described for panel A. Error bars represent the standard deviations from three independent experiments.

romosomal DNA from *E. coli*(pLA1) and *E. coli*(pLA1-ΔTnp) was isolated and used as the template in PCRs with IS*256*-specific, outward-directed primers (Fig. 7A). In this experiment, a specific 2.1-kb PCR product can be generated only if IS*256* forms an extrachromosomal DNA circle. Figure 7B shows the appearance of a band of 2.1 kb only in the extrachromosomal DNA fraction from *E. coli*(pLA1), indicating that IS*256*r transposase was able to excise the insertion sequence and produce circular intermediaries.

To determine whether the insertional activity of IS*256*r depends on the presence of σ^B, plasmid pLA1 was cloned in the *S. aureus* 15981 and $\Delta\sigma^B$ strains. The insertion frequency was quantified as the number of chromosomal insertion events of IS*256*r in each strain, as determined by the number of erythromycin-resistant/chloramphenicol-sensitive colonies (Fig. 7C). The colonies were expected to be chloramphenicol sensitive because we were screening for loss of the plasmid. The results showed a significant, 2.5-fold increase ($P < 0.01$) in the percentage of erythromycin-resistant/chloramphenicol-sensitive colonies obtained with the $\Delta\sigma^B$ strain compared to the percentage obtained with the wild-type strain. To confirm that the integration of IS*256*r in the chromosome was mediated by transposition activity and not by double crossover with chromosomal copies of IS*256*, Southern blotting was performed using IS*256*-specific and erythromycin-specific gene probes. The results revealed the appearance of new bands in the erythromycin-resistant/chloramphenicol-sensitive colony derivatives that hybridized with the IS*256* and erythromycin gene probes, suggesting integration of IS*256*r into the chromosome by transposition (Fig. 7D). Overall, these results indicate that the transpositional activity of IS*256*r is increased in the absence of σ^B.

Effect of culture media and temperature on the IS*256* activity of the $\Delta\sigma^B$ strain. To test whether environmental conditions affect the insertional activity of IS*256* in the $\Delta\sigma^B$ strain, we determined the number of biofilm phenotype variants of the 15981 and $\Delta\sigma^B$ strains on CRA plates and on TSA-milk after serial passage in different media (TSB, TSB-gluc, and TSB-NaCl [0.5 M]) and at different temperatures (30°C and 37°C). Interestingly, the presence of 0.5 M NaCl (or 0.5 M KCl [data not shown]) in the growth medium decreased the appearance of smooth and protease-overproducing variants in the $\Delta\sigma^B$ mutant to the levels in the wild type (Fig. 8). In contrast, a high frequency of biofilm phenotype variants was observed for the $\Delta\sigma^B$ mutant under the remaining conditions tested. From these results, we concluded that osmotic stress was able to compensate for the biofilm phenotype instability of the $\Delta\sigma^B$ mutant, suggesting that the activity of IS*256* was also regulated by environmental conditions. It is important to notice that the frequency of biofilm phenotypic variation slightly increased in the wild-type strain at 30°C (20%), strongly suggesting that

temperature plays a role in the biofilm phenotypic variation process.

Two-component systems (TCS) are the principal signal transducers involved in environmental sensing in *S. aureus*. Seventeen TCS have been annotated to occur in the *S. aureus* genome. Among them, *yycFG* is essential for cell viability, and SA0016-SA0017 is present only in methicillin-resistant strains. Thus, we investigated whether 15 isogenic mutations in TCS of the 15981 strain have effects on biofilm phenotypic variation. The results showed no changes in the frequency of appearance of smooth colonies under our experimental conditions (data not shown), indicating that the signals due to salt stress that induce IS*256* transposition activity are perceived by unknown mechanisms that are separate from TCS. Such signals might act directly to regulate the stability of the transposase transcript or transposase activity itself.

DISCUSSION

Biofilm formation in *S. aureus* is a tightly regulated process involving many different factors. In this regard, it has been reported that (i) IcaR is a strong negative regulator of *icaADBC* transcription, and in its absence, PIA/PNAG production and biofilm formation are enhanced (24); (ii) TcaR, a putative transcriptional regulator of the teicoplanin-associated locus, represses *icaADBC* transcription without affecting PIA/PNAG production (24); and (iii) SarA, a global virulence regulator, positively regulates *icaADBC* operon transcription and PIA/PNAG accumulation (4, 45). In parallel to this refined regulatory procedure, it has been shown that biofilm development in *S. aureus* and *S. epidermidis* is subject to an "all-or-none" control mechanism based on the integration/excision of the IS*256* insertion element in the *icaADBC* operon (9, 28, 48). IS*256* is a common element in the genomes of staphylococci and enterococci and is often present in multiple copies either flanking the Tn*4001* transposon or independent of it. Several studies have indicated that IS*256* elements are significantly more frequent in *S. epidermidis* strains of clinical origin than in commensal isolates, and the use of IS*256* as a genetic marker has been proposed (14, 19, 30, 42). Host cells have adopted different mechanisms for limiting the deleterious effects that uncontrolled transposition of insertion elements might cause (for a review, see Nagy and Chandler [38]). In the case of IS*256*, nothing was known about the mechanisms used by staphylococci to control IS*256* insertion/excision activity.

The results of our study revealed that the absence of the global stress response regulator σ^B increased the frequency of smooth colonies, completely reversing the balance of smooth/rough bacteria in the culture over a 7-day period. The molecular mechanism responsible for the change to smooth, biofilm-negative colonies in the σ^B mutant strain might involve either the activation of a new genetic mechanism of phenotypic variation or the increased transposition activity of the IS*256* element. Genetic analysis of biofilm-negative variants of the σ^B strain showed that insertion of IS*256* at different positions in the *icaC* gene occurs in 30% of the biofilm-negative variants. This percentage coincided with the frequencies already described for wild-type strains of *S. epidermidis*, strongly suggesting that similar mechanisms of biofilm phenotypic variation take place in the wild-type and σ^B strains. To demonstrate that the transposition of IS*256* increases in the absence of σ^B, the insertion frequency of IS*256*r, containing an erythromycin resistance gene, was determined. The results showed that the chromosomal insertion frequency of IS*256*r from a plasmid was almost three times higher in the σ^B mutant than in the parental strain. According to RT-PCR experiments, the absence of σ^B was not associated with an increased transcription of the transposase. Therefore, it appears that σ^B regulates the expression of an unknown element that, either alone or in concert with additional factors, represses the translation of IS*256* transposase mRNA or the transposase's enzymatic activity. Further studies are required to determine the molecular mechanism by which σ^B regulates IS*256* transposase activity.

The mechanisms of target recognition by the IS*256* transposase have not been characterized, but preferential insertion of IS*256* in the *icaC*, *rsbU*, and *sarA* genes has previously been reported to occur in *Staphylococcus epidermidis* (9, 48). In agreement with these results, we observed that the increased activity of IS*256* in the absence of σ^B did not influence target specificity, and the same preferential insertion of IS*256* in the *icaC* and *sarA* genes was observed among the $\Delta\sigma^B$-derived, biofilm-negative variants. *rsbU*, a positive activator of σ^B, was previously reported to accumulate 11% of the IS*256* insertions in biofilm-negative colonies (9). It has been shown that the absence of *rsbU* causes a reduction in σ^B activity; therefore, insertional inactivation of *rsbU* is expected to mimic σ^B mutation (40). The evolutionary selection of *rsbU* as a preferential IS*256* insertion site might represent a positive-feedback mechanism for increasing transposition activity under specific environmental conditions. This hypothesis is also supported by the finding that σ^B-deficient *S. aureus* strains occur frequently in nature (27). Indeed, we have observed that natural IS*256*-containing σ^B-negative isolates of *S. aureus* very often contained a very high copy number of the IS*256* element, suggesting that IS*256* activity is increased in naturally σ^B-deficient *S. aureus* strains (our unpublished results). We have not been able to determine the frequency of insertion of IS*256* into the *rsbU* gene because *rsbU*-deficient variants of *S. aureus*, in contrast to *S. epidermidis*, are effective biofilm producers that display rough colony morphology in CRA. An intriguing result relating to IS*256* target recognition is the enormous number of copies of IS*256* present in biofilm-negative variants that, in principle, should seriously compromise bacterial survival.

The high frequency of emergence of biofilm-negative variants in the σ^B mutant might also explain previous reports conferring opposite roles to σ^B in *S. aureus* biofilm formation (41, 45). It was first reported that the disruption of σ^B in the clinical strain MA12 impaired the biofilm formation capacity of the bacteria (41). Then, we reported that the deletion of σ^B from two genetically unrelated *S. aureus* strains did not affect biofilm formation capacity (45). It is likely that a biofilm-negative variant could be unconsciously selected during the mutagenesis procedure of σ^B in strain MA12 that would distort the observed phenotype. Similar conjectures might be applied to other studies that analyzed the effects of σ^B deficiency in bacterial biology. For example, one study investigated the effect of nutrient limitation on *S. epidermidis* biofilms (23). Biofilms of strain *S. epidermidis* 8400 with deletion of both *rsbU* and σ^B disintegrated within 2 to 3 days in TSB without glucose, whereas biofilms of mutants in negative regulators of σ^B

(RsbW) displayed high stability over at least 6 days. Based on these results, those authors concluded that the stability of established biofilms under conditions of nutrient limitation depends on σ^B activity (23). However, it is possible that the increased activity of IS*256* in the σ^B-deficient *S. epidermidis* 8400 strain might favor the appearance of biofilm-negative variants that caused the biofilm disintegration phenotype. To date, most of the studies investigating the role of σ^B in *S. aureus* have been performed using IS*256*-free *S. aureus* 8325-4 and COL strains; therefore, phenotypes would not be affected by this mobile element (8, 17, 18, 32). Nevertheless, it is important to keep in mind the potential influence of mobile elements when regulatory gene deficiencies are analyzed in natural bacterial isolates because transposon-mediated phase variation might underlie contradictory phenotypes associated with particular bacterial strains.

Growth conditions modulate the transposition activities of mobile elements by affecting the expression of transposition-related genes and/or their activities and/or of host factors that regulate transposition activity (38). In particular, stress situations such as carbon starvation, extreme temperature, and UV light have been correlated with the enhanced transposition of bacterial mobile elements (10, 15, 22, 31, 33, 39). These findings support the idea that bacteria derepress the movement of mobile elements as an adaptive response to stress and to permit new traits to evolve (6, 46). In contrast to this idea, we observed that σ^B, a global regulator that enables adaptation to environmental stresses, is a repressor of IS*256* activity. In this situation, environmental stress conditions would activate σ^B activity and decrease the generation of biofilm-negative variants. Accordingly, salt stress (NaCl or KCl), which has been shown to induce biofilm formation (41), represses IS*256* activity in the absence of σ^B, indicating that the sensor for osmotic stress influences IS*256* activity downstream of σ^B.

Direct consequences of the change in biofilm switching frequency and the enrichment of smooth colonies in the bacterial population are the progressive degradation of an established biofilm and the release of biofilm-negative variants that can colonize new niches. An enzymatic activity (dispersin B) able to degrade the PIA/PNAG exopolysaccharide matrix to facilitate bacterial detachment from biofilms has been described for *Actinobacillus actinomycetemcomitans* (25, 26). In the absence of a dispersin homologue in the *S. aureus* genome, it appears that the generation of an appropriate ratio of biofilm-negative variants through the insertion/excision activity of IS*256* plays an important role in controlling the transition from a biofilm to a planktonic lifestyle.

ACKNOWLEDGMENTS

Marta Vergara-Irigaray is a predoctoral fellow (FPU) from the Ministerio de Educación y Ciencia, Spain. Nekane Merino is a predoctoral fellow from the Basque Government, Spain. This work was supported by the BIO2005-08399 grant from the Spanish Ministerio de Educación y Ciencia and grant LSHM-CT-2006-019064 from the European Union.

We thank Susanne Hennig, Wilma Ziebuhr, Alejandro Toledo-Arana, Josep Casadesus, and Cristina Solano for critical reading of the manuscript.

REFERENCES

1. **Arnaud, M., A. Chastanet, and M. Débarbouillé.** 2004. A new vector for efficient allelic replacement in naturally nontransformable low GC% gram-positive bacteria. Appl. Environ. Microbiol. **70:**6887–6891.
2. **Arrizubieta, M. J., A. Toledo-Arana, B. Amorena, J. R. Penades, and I. Lasa.** 2004. Calcium inhibits Bap-dependent multicellular behavior in *Staphylococcus aureus*. J. Bacteriol. **186:**7490–7498.
3. **Ausubel, F. M., R. Brent, R. E. Kingston, D. D. Moore, J. G. Seidman, J. A. Smith, and K. Struhl (ed.).** 1990. Current protocols in molecular biology. John Wiley & Sons, New York, NY.
4. **Beenken, K. E., J. S. Blevins, and M. S. Smeltzer.** 2003. Mutation of *sarA* in *Staphylococcus aureus* limits biofilm formation. Infect. Immun. **71:**4206–4211.
5. **Bruckner, R.** 1997. Gene replacement in *Staphylococcus carnosus* and *Staphylococcus xylosus*. FEMS Microbiol. Lett. **151:**1–8.
6. **Capy, P., G. Gasperi, C. Biemont, and C. Bazin.** 2000. Stress and transposable elements: co-evolution or useful parasites? Heredity **85**(Part 2)**:**101–106.
7. **Chan, P. F., and S. J. Foster.** 1998. Role of SarA in virulence determinant production and environmental signal transduction in *Staphylococcus aureus*. J. Bacteriol. **180:**6232–6241.
8. **Chan, P. F., S. J. Foster, E. Ingham, and M. O. Clements.** 1998. The *Staphylococcus aureus* alternative sigma factor σ^B controls the environmental stress response but not starvation survival or pathogenicity in a mouse abscess model. J. Bacteriol. **180:**6082–6089.
9. **Conlon, K. M., H. Humphreys, and J. P. O'Gara.** 2004. Inactivations of *rsbU* and *sarA* by IS*256* represent novel mechanisms of biofilm phenotypic variation in *Staphylococcus epidermidis*. J. Bacteriol. **186:**6208–6219.
10. **Coros, A. M., E. Twiss, N. P. Tavakoli, and K. M. Derbyshire.** 2005. Genetic evidence that GTP is required for transposition of IS*903* and Tn*552* in *Escherichia coli*. J. Bacteriol. **187:**4598–4606.
11. **Costerton, J. W., P. S. Stewart, and E. P. Greenberg.** 1999. Bacterial biofilms: a common cause of persistent infections. Science **284:**1318–1322.
12. **Cramton, S. E., C. Gerke, N. F. Schnell, W. W. Nichols, and F. Gotz.** 1999. The intercellular adhesion (*ica*) locus is present in *Staphylococcus aureus* and is required for biofilm formation. Infect. Immun. **67:**5427–5433.
13. **Cucarella, C., C. Solano, J. Valle, B. Amorena, I. I. Lasa, and J. R. Penades.** 2001. Bap, a *Staphylococcus aureus* surface protein involved in biofilm formation. J. Bacteriol. **183:**2888–2896.
14. **Deplano, A., M. Vaneechoutte, G. Verschraegen, and M. J. Struelens.** 1997. Typing of *Staphylococcus aureus* and *Staphylococcus epidermidis* strains by PCR analysis of inter-IS*256* spacer length polymorphisms. J. Clin. Microbiol. **35:**2580–2587.
15. **Eichenbaum, Z., and Z. Livneh.** 1998 UV light induces IS10 transposition in *Escherichia coli*. Genetics **149:**1173–1181.
16. **Freeman, D. J., F. R. Falkiner, and C. T. Keane.** 1989. New method for detecting slime production by coagulase negative staphylococci. J. Clin. Pathol. **42:**872–874.
17. **Gertz, S., S. Engelmann, R. Schmid, A. K. Ziebandt, K. Tischer, C. Scharf, J. Hacker, and M. Hecker.** 2000. Characterization of the σ^B regulon in *Staphylococcus aureus*. J. Bacteriol. **182:**6983–6991.
18. **Giachino, P., S. Engelmann, and M. Bischoff.** 2001. σ^B activity depends on RsbU in *Staphylococcus aureus*. J. Bacteriol. **183:**1843–1852.
19. **Gu, J., H. Li, M. Li, C. Vuong, M. Otto, Y. Wen, and Q. Gao.** 2005. Bacterial insertion sequence IS*256* as a potential molecular marker to discriminate invasive strains from commensal strains of *Staphylococcus epidermidis*. J. Hosp. Infect. **61:**342–348.
20. **Hall-Stoodley, L., and P. Stoodley.** 2005. Biofilm formation and dispersal and the transmission of human pathogens. Trends Microbiol. **13:**7–10.
21. **Heilmann, C., O. Schweitzer, C. Gerke, N. Vanittanakom, D. Mack, and F. Gotz.** 1996. Molecular basis of intercellular adhesion in the biofilm-forming *Staphylococcus epidermidis*. Mol. Microbiol. **20:**1083–1091.
22. **Ilves, H., R. Horak, and M. Kivisaar.** 2001. Involvement of σ^S in starvation-induced transposition of *Pseudomonas putida* transposon Tn*4652*. J. Bacteriol. **183:**5445–5448.
23. **Jager, S., D. Mack, H. Rohde, M. A. Horstkotte, and J. K. Knobloch.** 2005. Disintegration of *Staphylococcus epidermidis* biofilms under glucose-limiting conditions depends on the activity of the alternative sigma factor σ^B. Appl. Environ. Microbiol. **71:**5577–5581.
24. **Jefferson, K. K., D. B. Pier, D. A. Goldmann, and G. B. Pier.** 2004. The teicoplanin-associated locus regulator (TcaR) and the intercellular adhesin locus regulator (IcaR) are transcriptional inhibitors of the *ica* locus in *Staphylococcus aureus*. J. Bacteriol. **186:**2449–2456.
25. **Kaplan, J. B., C. Ragunath, K. Velliyagounder, D. H. Fine, and N. Ramasubbu.** 2004. Enzymatic detachment of *Staphylococcus epidermidis* biofilms. Antimicrob. Agents Chemother. **48:**2633–2636.
26. **Kaplan, J. B., K. Velliyagounder, C. Ragunath, H. Rohde, D. Mack, J. K. Knobloch, and N. Ramasubbu.** 2004. Genes involved in the synthesis and degradation of matrix polysaccharide in *Actinobacillus actinomycetemcomitans* and *Actinobacillus pleuropneumoniae* biofilms. J. Bacteriol. **186:**8213–8220.

27. **Karlsson-Kanth, A., K. Tegmark-Wisell, S. Arvidson, and J. Oscarsson.** 2006. Natural human isolates of *Staphylococcus aureus* selected for high production of proteases and alpha-hemolysin are sigma(B) deficient. Int. J. Med. Microbiol. **296:**229–236.
28. **Kiem, S., W. S. Oh, K. R. Peck, N. Y. Lee, J. Y. Lee, J. H. Song, E. S. Hwang, E. C. Kim, C. Y. Cha, and K. W. Choe.** 2004. Phase variation of biofilm formation in *Staphylococcus aureus* by IS 256 insertion and its impact on the capacity adhering to polyurethane surface. J. Korean Med. Sci. **19:**779–782.
29. **Knobloch, J. K., K. Bartscht, A. Sabottke, H. Rohde, H. H. Feucht, and D. Mack.** 2001. Biofilm formation by *Staphylococcus epidermidis* depends on functional RsbU, an activator of the *sigB* operon: differential activation mechanisms due to ethanol and salt stress. J. Bacteriol. **183:**2624–2633.
30. **Kozitskaya, S., S. H. Cho, K. Dietrich, R. Marre, K. Naber, and W. Ziebuhr.** 2004. The bacterial insertion sequence element IS*256* occurs preferentially in nosocomial *Staphylococcus epidermidis* isolates: association with biofilm formation and resistance to aminoglycosides. Infect. Immun. **72:**1210–1215.
31. **Kretschmer, P. J., and S. N. Cohen.** 1979. Effect of temperature on translocation frequency of the Tn*3* element. J. Bacteriol. **139:**515–519.
32. **Kullik, I., P. Giachino, and T. Fuchs.** 1998. Deletion of the alternative sigma factor σ^B in *Staphylococcus aureus* reveals its function as a global regulator of virulence genes. J. Bacteriol. **180:**4814–4820.
33. **Lamrani, S., C. Ranquet, M. J. Gama, H. Nakai, J. A. Shapiro, A. Toussaint, and G. Maenhaut-Michel.** 1999. Starvation-induced Mucts62-mediated coding sequence fusion: a role for ClpXP, Lon, RpoS and Crp. Mol. Microbiol. **32:**327–343.
34. **Loessner, I., K. Dietrich, D. Dittrich, J. Hacker, and W. Ziebuhr.** 2002. Transposase-dependent formation of circular IS*256* derivatives in *Staphylococcus epidermidis* and *Staphylococcus aureus*. J. Bacteriol. **184:**4709–4714.
35. **Mack, D., W. Fischer, A. Krokotsch, K. Leopold, R. Hartmann, H. Egge, and R. Laufs.** 1996. The intercellular adhesin involved in biofilm accumulation of *Staphylococcus epidermidis* is a linear beta-1,6-linked glucosaminoglycan: purification and structural analysis. J. Bacteriol. **178:**175–183.
36. **Maira-Litran, T., A. Kropec, C. Abeygunawardana, J. Joyce, G. Mark III, D. A. Goldmann, and G. B. Pier.** 2002. Immunochemical properties of the staphylococcal poly-*N*-acetylglucosamine surface polysaccharide. Infect. Immun. **70:**4433–4440.
37. **McKenney, D., K. Pouliot, V. Wang, V. Murthy, M. Ulrich, G. Döring, J. C. Lee, D. A. Goldmann, and G. B. Pier.** 1999. Broadly protective vaccine for *Staphylococcus aureus* based on an in vivo-expressed antigen. Science **284:**1523–1527.
38. **Nagy, Z., and M. Chandler.** 2004. Regulation of transposition in bacteria. Res. Microbiol. **155:**387–398.
39. **Ohtsubo, Y., H. Genka, H. Komatsu, Y. Nagata, and M. Tsuda.** 2005. High-temperature-induced transposition of insertion elements in *Burkholderia multivorans* ATCC 17616. Appl. Environ. Microbiol. **71:**1822–1828.
40. **Palma, M., and A. L. Cheung.** 2001. σ^B activity in *Staphylococcus aureus* is controlled by RsbU and an additional factor(s) during bacterial growth. Infect. Immun. **69:**7858–7865.
41. **Rachid, S., K. Ohlsen, U. Wallner, J. Hacker, M. Hecker, and W. Ziebuhr.** 2000. Alternative transcription factor σ^B is involved in regulation of biofilm expression in a *Staphylococcus aureus* mucosal isolate. J. Bacteriol. **182:**6824–6826.
42. **Rohde, H., M. Kalitzky, N. Kroger, S. Scherpe, M. A. Horstkotte, J. K. Knobloch, A. R. Zander, and D. Mack.** 2004. Detection of virulence-associated genes not useful for discriminating between invasive and commensal *Staphylococcus epidermidis* strains from a bone marrow transplant unit. J. Clin. Microbiol. **42:**5614–5619.
43. **Stewart, P. S., and J. W. Costerton.** 2001. Antibiotic resistance of bacteria in biofilms. Lancet **358:**135–138.
44. **Tormo, M. A., M. Marti, J. Valle, A. C. Manna, A. L. Cheung, I. Lasa, and J. R. Penades.** 2005. SarA is an essential positive regulator of *Staphylococcus epidermidis* biofilm development. J. Bacteriol. **187:**2348–2356.
45. **Valle, J., A. Toledo-Arana, C. Berasain, J. M. Ghigo, B. Amorena, J. R. Penades, and I. Lasa.** 2003. SarA and not σ^B is essential for biofilm development by *Staphylococcus aureus*. Mol. Microbiol. **48:**1075–1087.
46. **Wessler, S. R.** 1996. Turned on by stress. Plant retrotransposons. Curr. Biol. **6:**959–961.
47. **Ziebuhr, W.** 2001. *Staphylococcus aureus* and *Staphylococcus epidermidis*: emerging pathogens in nosocomial infections. Contrib. Microbiol. **8:**102–107.
48. **Ziebuhr, W., V. Krimmer, S. Rachid, I. Lossner, F. Gotz, and J. Hacker.** 1999. A novel mechanism of phase variation of virulence in *Staphylococcus epidermidis*: evidence for control of the polysaccharide intercellular adhesin synthesis by alternating insertion and excision of the insertion sequence element IS256. Mol. Microbiol. **32:**345–356.